Thermochimica Acta, 196 (1992) 379–389
Elsevier Science Publishers B.V., Amsterdam

Solid-state non-isothermal kinetics of sulfonamide–ammonia adduct desolvation

Christy M. Wyandt [1] and Douglas R. Flanagan

Pharmaceutics Department, College of Pharmacy, University of Iowa, Iowa City, IA 52242 (USA)

(Received 28 June 1991)

Abstract

A general differential technique is proposed for obtaining non-isothermal kinetic information from thermogravimetric data. This method uses a differential form of the general non-isothermal kinetic expression and fits desolvation data to rate laws corresponding to each of 11 solid-state mechanisms. The correct mechanism is determined to be the one the data fit most closely and the activation energy is calculated for this rate law. The method was used to evaluate the desolvation of six sulfonamide–ammonia adducts. A correlation was found between the calculated isothermal activation energies for a drug and its pK_a. Sulfonamides with higher pK_a values had lower desolvation activation energies and those with lower pK_a values had higher desolvation activation energies.

INTRODUCTION

Many techniques for obtaining kinetic information from non-isothermal thermogravimetric analysis have been proposed and are summarized in several review articles [1–6]. Unfortunately, there is now no clear consensus as to which method is the most appropriate for use in the study of desolvation and no real understanding of the significance of the extracted kinetic parameters. This study was undertaken to develop a general method for performing non-isothermal kinetic analyses and to use this technique to study the desolvation of a series of very similar compounds: the sulfonamide–ammonia adducts. An investigation of the non-isothermal kinetics of desolvation of these adducts should provide insight into the significance of the calculated activation energy.

[1] Current address: Pharmaceutics Department, Research Institute of Pharmaceutical Sciences, School of Pharmacy, University of Mississippi, University, MS 38677, USA.

EXPERIMENTAL

Materials and instruments

Sulfamethizole, sulfamerazine, sulfisoxazole, sulfamoxole, sulfisomidine and sulfamethazine were all obtained from Sigma Chemical Company, St. Louis, MO. Ammonia gas was obtained from Matheson Gases, Joliet, IL. Thermogravimetric analysis was conducted using a TGS-2 thermogravimetric analyzer interfaced with a Model 3600 data station with a TADS-1 plotter, all manufactured by Perkin–Elmer of Norwalk, CT.

Adduct preparation

To prepare the adducts, approximately one gram of drug was placed in the bottom of a 250 milliliter Erlenmeyer flask. Parafilm® was placed over the mouth of the flask leaving only a small opening. The flask was purged with ammonia and then, with the gas still flowing, the flask was transferred to an acetone–dry-ice bath where the gas liquified and dissolved the drug. When all the drug was dissolved in the ammonia, the flask was transferred to an ice bath to allow excess ammonia to evaporate. When evaporation was complete, the flasks were sealed and stored at approximately 5 °C.

Thermogravimetric analysis

TGA data were collected using a Perkin–Elmer TGS-2 thermogravimetric analyzer connected to a Perkin–Elmer Model 3600 data station. Data were recorded in a computer file on the data station and transferred to a floppy disk at the end of the experimental run. Data were collected at a heating rate of 5 °C min^{-1} using samples of approximately 10 mg; a constant nitrogen purge was maintained through each run.

Weight loss was calculated using the TADS TGA standard program. Weight loss was measured from the temperature at which the thermogram departed form the baseline to the temperature at which the new baseline was established.

DESCRIPTION OF KINETIC TECHNIQUE EMPLOYED

After systematically evaluating the computational techniques available for non-isothermal kinetic analysis of desolvation, an appropriate method for performing the computation was developed. For this solution, the general non-isothermal kinetic equation

$$\frac{d\alpha}{dT} = \frac{K(T)}{a} f(\alpha) \tag{1}$$

TABLE 1

Solid state mechanisms and rate laws

Type of process	Mechanism	Rate law
Phase boundary movement	R1	$(1-\alpha)^0$
Phase boundary movement	R2	$2(1-\alpha)^{1/2}$
Phase boundary movement	R3	$3(1-\alpha)^{2/3}$
Bulk growth of nuclei	F1	$(1-\alpha)$
Bulk growth of nuclei	A2	$2(1-\alpha)(-\ln(1-\alpha))^{1/2}$
Bulk growth of nuclei	A3	$3(1-\alpha)(-\ln(1-\alpha))^{2/3}$
Bulk growth of nuclei	A4	$4(1-\alpha)(-\ln(1-\alpha))^{3/4}$
Diffusion	D1	α^{-1}
Diffusion	D2	$(-\ln(1-\alpha))^{-1}$
Diffusion	D3	$(3/2)(1-\alpha)^{2/3}((1-\alpha)^{-1/3}-1)$
Diffusion	D4	$(3/2)(1-\alpha)^{-1/3}-1)^{-1}$

was linearized using a differential solution as introduced by Freeman and Carroll [7] and used by Abou-Shaaban and Simonelli [8] and others. The general form of this solution is

$$\ln\left(\frac{d\alpha/dT}{f(\alpha)}\right) = \ln\left(\frac{Z}{a}\right) - \frac{E_a}{RT} \tag{2}$$

Using this form of the kinetic equation, the data are fit to each of 11 rate laws corresponding to the solid state mechanisms summarized in Table 1. Satava [9] suggested these mechanisms as the most likely for solid state processes. The correct mechanism is assumed to be the one which results in the best correlation coefficient for the fit. The activation energy is then the one calculated for that model. Two computer programs were written for the Perkin–Elmer TADS to perform the calculations.

To begin the calculation, the user enters the weights corresponding to the initiation and conclusion of the transformation. The program calculates α and $1/T$ for a 10–90% conversion range. The term α is defined as

$$\alpha = \frac{W(0) - W(t)}{W(0) - W(f)} \tag{3}$$

The term $W(0)$ is the initial sample weight, $W(t)$ is the weight at time t, and $W(f)$ is the weight when the transformation is complete. The derivative $d\alpha/dT$ is determined by fitting three adjacent (α, T) pairs to a straight line using linear regression; $d\alpha/dT$ at the midpoint of the three is assumed to be the slope of the line. These calculated terms are then fit to each of the models using linear regression. The activation energy is then calculated from the slope of the linear fit for each model. A major criticism of the differential technique is that it requires that the derivative of the weight loss curve be determined, which may increase experimental scatter. How-

ever, this problem should be minimized by using the proper computational technique.

Other techniques for determining the derivative of the weight loss curve were evaluated. These include fitting the data to be a spline function, a second-order polynomial and a third-order polynomial. For these solutions, the derivative of the function at a given point was taken as the derivative of the weight loss curve at that point. Taking the derivative of a spline function was determined to introduce significant scatter in the calculated derivative. This is because although for desolvation the weight should always decrease, electronic scatter may interfere, resulting in an apparent increase in weight. A spline function fits the data exactly, so this increase would be reflected by an inaccurate derivative. The derivatives of the second- and third-order polynomials were in excellent agreement with those of the straight line. Because the linear fit is adequate and faster to compute, it was selected for the derivative evaluation.

The primary advantage to this type of differential solution is that the results should be relatively free from procedural effects as shown by Abou-Shaaban and Simonelli [8]. They assert that procedural effects upon calculated kinetic parameters are due to thermal gradients in the sample and that this effect can be minimized by dividing the derivative of the weight loss curve by $f(\alpha)$.

EVALUATION OF SELECTED TECHNIQUE

Before the kinetic method and corresponding computer program could be used with confidence, a series of tests were performed to evaluate them. The first evaluation used simulated data. A program was written to simulate data using a fourth-order Runge–Kutta method. The model, the activation energy and the pre-exponential divided by the heating rate were the variables used for the simulation. The simulated data were then evaluated using the mechanism selection and activation energy calculation programs.

To evaluate the mechanism selection program, data were simulated using each of the 11 models. The program was run and the appropriate model selected for each simulation. The results of these simulations and calculations appear in Table 2. It should be noted that in most cases the program selected the correct model for the simulated data. The rate laws for the nucleation models, F1, A4, A3 and A2, become virtually indistinguishable when the logarithm of their mathematical expressions is taken, as do the rate laws for models R3 and R2. Therefore, when data appear to follow one of these models, other methods must be employed to insure the correct mechanism selection.

Next, the simulated data were kinetically evaluated and the results plotted. The model used for the simulation was the same as the one used

TABLE 2

Evaluation of the mechanism selection program using simulated data. Data simulated for $E_a = 30$ kcal mol^{-1}

Model for simulation	Mechanism selected	E_a (kcal mol^{-1})
F1	F1, A4, A3, A2	29.9, 6.0, 8.7, 14.0
D4	D4	29.9
D3	D3	29.7
D2	D2	29.8
D1	D1	29.8
R3	R3, R2	32.0, 31.0
R2	R2, R3	29.7, 33.0
R1	R1	29.8
A4	A4, A3, A2, F1	28.8, 39.5, 60.8, 124.8
A3	A3, A4, A2, F1	29.5, 20.9, 46.8, 98.6
A2	A2, A4, A3, F1	29.8, 11.0, 17.2, 67.3

for the evaluation. An example of a plot for the simulated data appears in Fig. 1. The data for this model were simulated using model D3 and an activation energy of 90 kcal mol^{-1}. The results of the calculation appear to be in very good agreement with the input parameters for the simulation.

The results of the evaluation of the simulated data sets indicate that the computer programs were operating properly. Some further evaluations

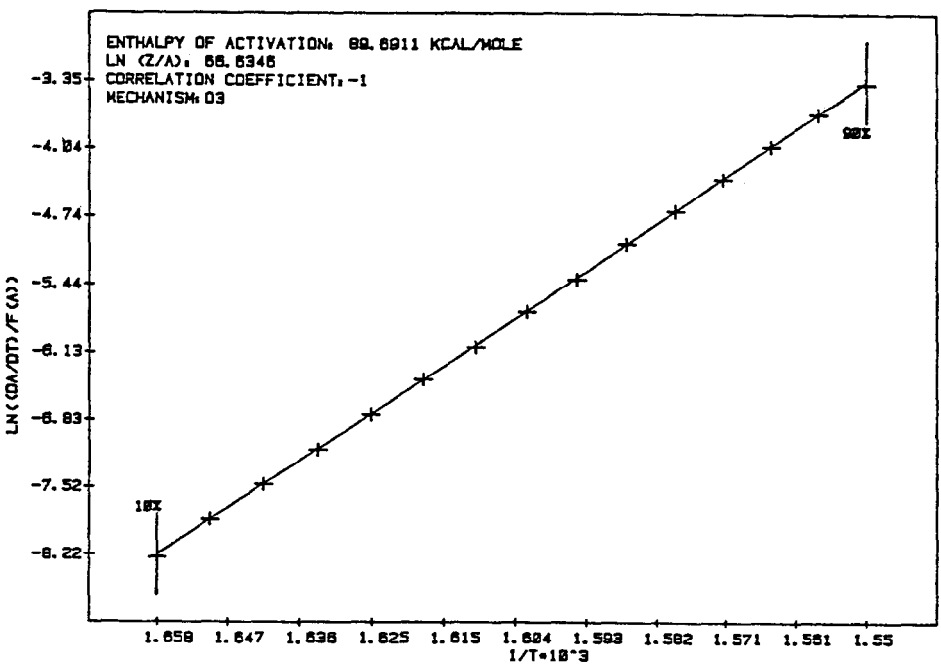

Fig. 1. Arrhenius plot for data simulated and evaluated using model D3.

TABLE 3

Effect of varying the percentage conversion range on the mechanism selection for sulfamethizole–ammonia adduct

Mechanism	Conversion range			
	25–75%		10–90%	
	E_a (kcal mol^{-1})	r	E_a (kcal mol^{-1})	r
F1	85.1	−0.94	82.5	−0.93
D4	127.2	−0.97	125.9	−0.94
D3	149.2	−0.98	148.2	−0.96
D2	115.8	−0.97	114.1	−0.91
D1	86.9	−0.94	85.9	−0.83
R3	63.1	−0.91	60.1	−0.86
R2	52.1	−0.88	48.9	−0.79
R1	19.1	−0.55	15.4	−0.32
A4	12.6	−0.39	8.4	−0.27
A3	20.7	−0.57	16.7	−0.48
A2	36.2	−0.77	33.1	−0.74

were required to determine whether the method was robust enough to be used for experimental data.

For the next series of evaluations, experimental data were used. The range of percent conversion was varied in order to determine the effect on the calculated activation energy or the selected mechanism for the data set. To evaluate the effect of percentage conversion on mechanism selection, a data set for desolvation of the sulfamethizole–ammonia adduct was used. The results of this calculation are summarized in Table 3. The mechanism selected for the 25–75% conversion range is the same D3 mechanism. This indicates that 10–90% conversion is an appropriate range for selecting a mechanism.

To evaluate the effect of varying percent conversion range on the calculated activation energy, a sulfamethazine–ammonia adduct desolvation data set was evaluated and the range varied for the calculation. For this set of data, the general program selected mechanism D3 as the most appropriate for the calculations. The results of this study appear in Table 4.

TABLE 4

Effect of varying percentage conversion range on calculated E_a for sulfamethazine–ammonia adduct deammoniation

E_a (kcal mol^{-1})	r	% Conversion range
46.9	−0.94	10–60
45.9	−0.95	20–80
45.3	−0.94	40–80
46.7	−0.92	25–75

These results indicate that calculation of activation energy is generally independent of the range of percent conversion used for the calculation. This means that the D3 model used for the calculation fits the data equally well over the 10–90% conversion ranges as it does for the smaller ranges. This supports both the selection of the D3 model and the use of a 10–90% conversion range for the calculation.

KINETIC EVALUATION OF SULFONAMIDE–AMMONIA ADDUCTS

The kinetics of desolvation of the six sulfonamide–ammonia adducts was non-isothermally investigated using the general differential technique as described. Table 5 gives the results of the general fit program for sulfamoxole, a representative sulfonamide. Figures 2 and 3 show the corresponding TGA thermogram for sulfamoxole–ammonia adduct desolvation and the kinetic plot. The data were plotted using the mechanism which resulted in the highest correlation coefficient as indicated by the general fit program.

The mechanism selected for all the adducts was D3, a three-dimensional diffusion model. This model was developed assuming that diffusion is the rate-limiting step. The process being investigated is desolvation, which requires that evolved gases diffuse through and leave the particle before weight loss is recorded; thus, the D3 mechanism is a plausible selection.

Table 6 lists calculated activation energies for the six sulfonamide–ammonia adducts. The activation energies are calculated for models F1, D3, and R3. Model F1 gives the best fit of the nucleation models, D3 of the diffusion models, and R3 of the geometric contraction models. Although the magnitude of the activation energies is different when different models are used, their rank ordering remains essentially the same.

Table 7 gives pK_a values and activation energies calculated using model D3 for the sulfonamide–ammonia adducts. The activation energies are the

TABLE 5

General fit program results for sulfamoxole–ammonia adduct desolvation

Mechanism	E_a (kcal mol^{-1})	Correlation coefficient
F1	28.6	−0.942
D4	42.8	−0.952
D3	49.8	−0.976
D2	39.1	−0.936
D1	30.4	−0.874
R3	21.7	−0.886
R2	18.2	−0.835
R1	7.7	−0.467
A4	5.0	−0.446
A3	7.7	−0.603
A2	12.9	−0.786

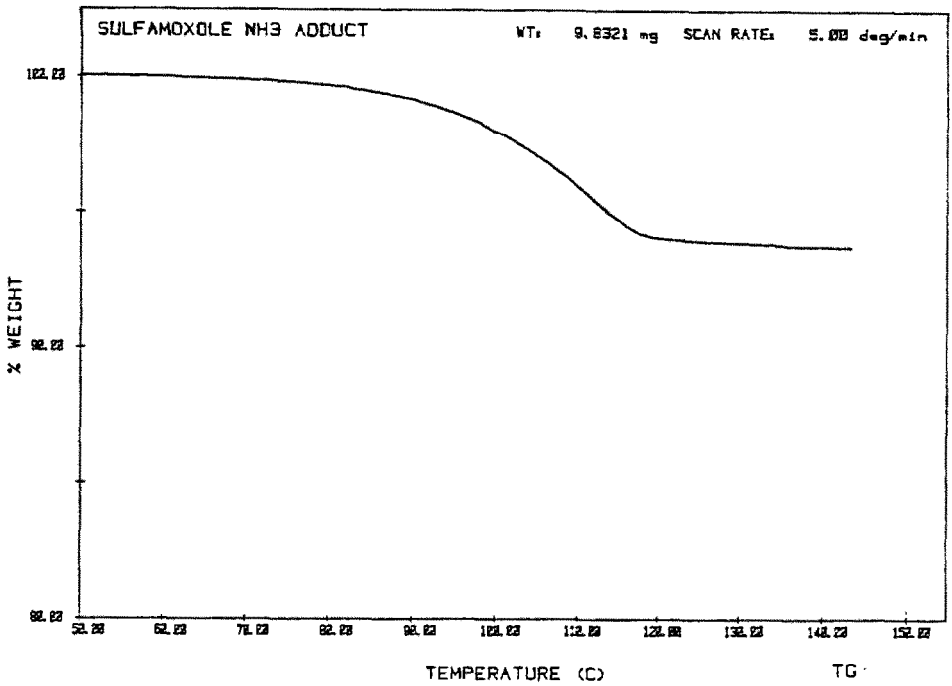

Fig. 2. TGA thermogram for sulfamoxole–ammonia adduct.

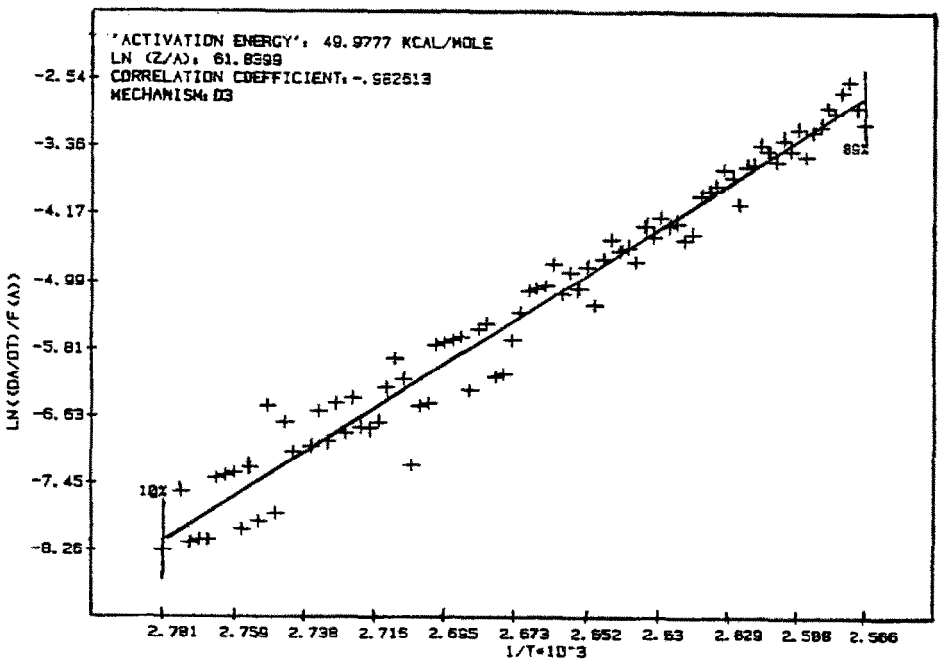

Fig. 3. Arrhenius plot for sulfamoxole–ammonia adduct.

TABLE 6
Calculated activation energies (kcal mol^{-1}) for various mechanisms for sulfonamide–ammonia adduct desolvation

Ammonia adduct	E_a for D3	E_a for R3	E_a for F1
Sulfisoxazole	150.8	78.0	93.3
Sulfamethizole	137.5	57.3	75.8
Sulfamerazine	49.8	19.1	26.3
Sulfamoxole	49.5	21.7	28.6
Sulfisomidine	43.9	23.9	28.3
Sulfamethazine	41.5	19.3	24.0

average of the results for two runs for each adduct. For the drugs with higher activation energies (i.e. sulfamethizole and sulfisoxazole) there was considerable variation in the calculated values for replicate runs.

The drugs with lower pK_a values have higher activation energies, and those with higher pK_a values have lower activation energies. The interaction between sulfonamides and ammonia is likely to be an acid–base-type occurring between the SO_2–NH–proton on the sulfonamide and the N on ammonia; therefore this correlation is significant. The pK_a of the parent drug should affect the strength of the ammonia–drug interaction, and this is reflected in the calculated activation energies. A sulfonamide with a low pK_a should interact more strongly with basic ammonia than a sulfonamide with a higher pK_a. A stronger drug–ammonia interaction should result in a higher calculated activation energy for desolvation. This correlates with the results of the kinetic analysis for the series of sulfonamides investigated.

The pK_a of a sulfonamide in water is used as a measure of its ability to share its proton with ammonia. Lowrey and Richardson [10] discuss the difficulties involved in relating acidities determined in different solvent systems and the gas phase. It is proposed that the relative acidities of the sulfonamides as described by the solution pK_a values are related to the

TABLE 7
Calculated activation energies for sulfonamide–ammonia adducts using model D3 and pK_a values of the sulfonamides

Ammonia adduct	Sulfonamide pK_a	E_a (kcal mol^{-1})
Sulfisoxazole	4.9	150.8
Sulfamethizole	5.4	137.5
Sulfamerazine	7.0	49.8
Sulfamoxole	7.4	49.5
Sulfisomidine	7.5	43.9
Sulfamethazine	7.7	41.5

TABLE 8

Linear regression results for sulphonamide–ammonia adduct desolvation activation energies correlated with pK_a

Model	Intercept	Slope	r
D3	4.55	−3.55	−0.989
R3	4.68	−3.69	−0.967
F1	4.60	−3.60	−0.981

strength of the sulfonamide–ammonia interaction, which should be correlated with gas-phase acidities if such data were available.

A linear regression was performed on normalized data for the models D3, R3, and F1. For the fit, $E_a/\overline{E}_a$ was the dependent variable and $pK_a/\overline{pK_a}$ was the independent variable. The results of this regression analysis for each model are given in Table 8. There is a significant linear correlation between E_a and pK_a for each model, with the best correlation observed for the D3 model.

For each model, the slope of the linear fit was close to −3.5. This indicates that calculated activation energies are highly dependent upon pK_a. The sulfonamides are all structurally similar in the region of interaction with ammonia, so steric effects are not expected. This high correlation between pK_a and E_a indicates that, in fact, steric factors are unimportant in assessing the strength of the sulfonamide–ammonia interaction.

This correlation between pK_a and calculated E_a is significant because it means that using this technique for calculating non-isothermal activation energies results in values that can be related to intrinsic properties of the compound involved. It is proposed that the non-isothermal activation energy is directly related to the strength of the sulfonamide–ammonia interaction.

CONCLUSION

This evaluation has shown that a general differential non-isothermal kinetic technique can be used successfully to study desolvation. This method was shown to yield calculated non-isothermal desolvation activation energies which can be related to other physicochemical parameters. This shows that meaningful kinetic information can be obtained using this calculation technique.

ACKNOWLEDGEMENT

This work was supported by a fellowship from the United States Pharmacopoeial Convention.

REFERENCES

1 J. Šesták, Silikaty, 11 (1967) 153.
2 J.H. Flynn and C.A. Wall, J. Res. Natl. Bur. Stand. Sect. A, 70 (1966) 487.
3 J. Šesták, V. Satava and W.W. Wendlandt, Thermochim. Acta, 7 (1973) 333.
4 W.W. Wendlandt, in P.J. Elving and J.D. Winefordner (Eds.), Thermal Analysis, 3rd edn., Wiley, New York, 1986, Chapt. 2.
5 N.J. Carr and A.K. Galwey, Thermochim. Acta, 79 (1983) 323.
6 C.D. Doyle, in P.E. Slade and L.T. Jenkins (Eds.), Techniques and Methods of Polymer Evaluation, Marcel-Dekker, New York, 1966, Chapt. 4.
7 E.S. Freeman and B. Carroll, J. Phys. Chem., 82 (1958) 394.
8 R.R.A. Abou-Shaaban and A.P. Simonelli, Thermochim. Acta, 26 (1978) 89.
9 V. Satava, Thermochim. Acta, 2 (1971) 423.
10 T.H. Lowrey and K.S. Richardson, Mechanism and Theory in Organic Chemistry, 2nd edn., Harper and Row, New York, 1981, Chapt. 3.